Biol. Cybern. 66, 389–397 (1992)

Biological Cybernetics

Simulating vestibular compensation using recurrent back-propagation

Thomas J. Anastasio

Department of Physiology and Biophysics and Beckman Institute, University of Illinois, 405 North Mathews Avenue, Urbana, IL 61801, USA

Received July 3, 1991/Accepted in revised form October 25, 1991

Abstract. Vestibular compensation is simulated as learning in a dynamic neural network model of the horizontal vestibulo-ocular reflex (VOR). The bilateral, three-layered VOR model consists of nonlinear units representing horizontal canal afferents, vestibular nuclei (VN) neurons and eye muscle motoneurons. Dynamic processing takes place via commissural connections that link the VN bilaterally. The intact network is trained, using recurrent back-propagation, to produce the VOR with velocity storage integration. Compensation is simulated by removing vestibular afferent input from one side and retraining the network. The time course of simulated compensation matches that observed experimentally. The behavior of model VN neurons in the compensated network also matches real data, but only if connections at the motoneurons, as well as at the VN, are allowed to be plastic. The dynamic properties of real VN neurons in compensated and normal animals are found to differ when tested with sinusoidal but not with step stimuli. The model reproduces these conflicting data, and suggests that the disagreement may be due to VN neuron nonlinearity.

Introduction

Vestibular compensation is one of the oldest and most well studied paradigms in motor learning (Schaefer and Meyer 1974). It is the process whereby the normal functioning of vestibular responses is wholly or partially regained following removal of one of the paired vestibular receptors. Although vestibular compensation has been well described behaviorally and neurophysiologically, the neural mechanisms underlying this important form of plasticity have yet to be completely understood.

Vestibular function is evaluated by analyzing the vestibulo-ocular reflex (VOR). The VOR stabilizes gaze by producing eye rotations that counterbalance head rotations. It is centered on brainstem neurons in the vestibular nuclei (VN) that relay head velocity signals from semicircular canal afferent neurons to the motoneurons of the eye muscles (Wilson and Melvill Jones 1979). The brainstem VOR circuitry also processes the canal signals, increasing their time constants from about five seconds in monkeys (Buttner and Waespe 1981) to about 20 s (Raphan et al. 1979) before transmitting this signal to the motoneurons. This process is known as velocity storage (ibid.).

The VOR is a bilaterally symmetric, reciprocal structure. Velocity storage may be mediated by the inhibitory commissural connections that link the VN bilaterally (Blair and Gavin 1981). Removal of the vestibular receptors from one side (hemilabyrinthectomy) unbalances the VOR, resulting in continuous eye movement that occurs in the absence of head movement, a condition known as spontaneous nystagmus. Such a lesion also reduces VOR sensitivity (gain) and eliminates velocity storage. Compensatory restoration of VOR occurs in stages (Wolfe and Kos 1977; Maioli et al. 1983; Fetter and Zee 1988). It begins by quickly eliminating spontaneous nystagmus, and continues by increasing VOR gain. Paradoxically, recovery of velocity storage is minimal.

A previous model (Galiana et al. 1984) identified many of the connections involved in vestibular compensation at the level of the bilateral VN. That model, however, was static and linear, and compensation was simulated by making arbitrary connection weight changes. The purpose of this study is to simulate compensation in a dynamic, nonlinear model of the VOR,

Abbreviations: AC, acutely lesioned network, before compensation; GR, gain restored, compensating network; *lb*, left bias (left nonvestibular input unit); *lhc*, left horizontal canal afferent (left input unit); *lr*, lateral rectus motoneuron (left output unit); *lvn1, 2*, left vestibular nuclei neurons (left hidden units); *mr*, medial rectus motoneuron (right output unit); NE, nystagmus eliminated, compensating network; NM, normal network, intact and fully trained; pass, one, input/desired-output training sequence presentation; *rb*, right bias (right nonvestibular input unit); *rhc*, right horizontal canal afferent (right input unit); *rvn1, 2*, right vestibular nuclei neurons (right hidden units); SR, spontaneous rate; tick, one time step of network processing (one cycle); VOR, vestibulo-ocular reflex; VN, vestibular nuclei

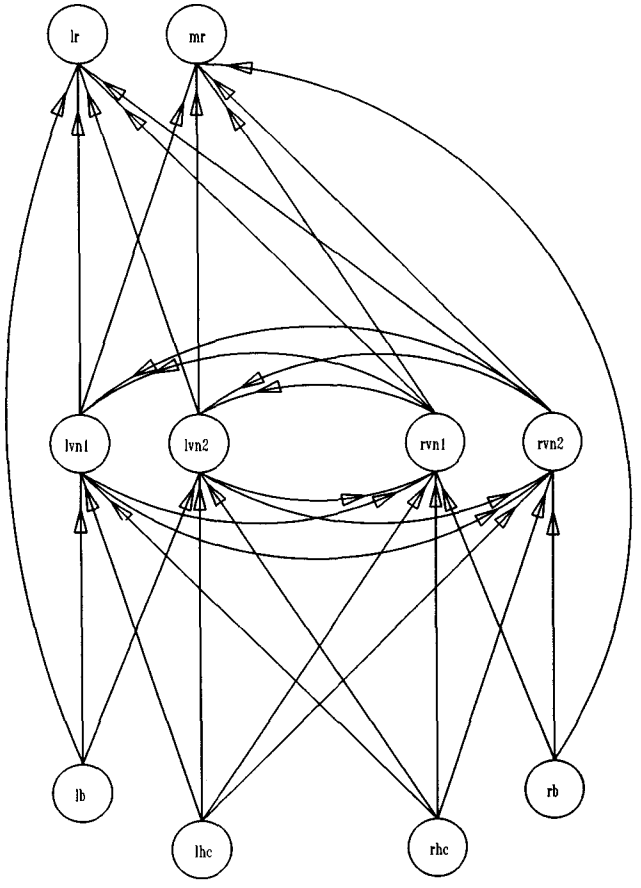

Fig. 1. Recurrent neural network model of the horizontal vestibulo-ocular reflex (VOR). *lhc*, *rhc*: left and right horizontal canal afferents (input units); *lvn1*, *lvn2*, *rvn1*, *rvn2*: vestibular nuclei neurons on the left and right sides of the model brainstem (hidden units); *lr*, *mr*: motoneurons of the lateral and medial rectus muscles of the left eye (output units); *lb*, *rb*: left and right nonvestibular inputs (bias units)

wherein the weights are changed objectively using a neural network learning algorithm. By adjusting network parameters to match better the model and actual data, hypotheses concerning the synaptic basis of vestibular compensation can be developed. Also, because the model is neurally based, it can explain some of the paradoxical phenomenology of the VOR in normal and compensated animals.

Network architecture

The horizontal VOR is modeled as a three-layered neural network, with two each of input, output and bias units and four hidden units (Fig. 1). All of the units are nonlinear, computing the weighted sum of their inputs and passing it through the sigmoidal squashing function (Rumelhart et al. 1986). As such, the units have an approximately linear response for midrange input sums, but are asymptotically driven into saturation (one) or cut-off (zero) for large positive or negative net inputs, respectively. Unit responses are 0.50 for net inputs of zero. Input units represent afferents from the left (*lhc*) and right (*rhc*) horizontal canal receptors. Output units correspond to motoneurons of the lateral (*lr*) and medial (*mr*) rectus muscles of the left eye. Neurons in the VN are represented by hidden units on the left (*lvn1*, *lvn2*) and right (*rvn1*, *rvn2*) sides of the model brainstem. Bias units stand for nonvestibular inputs, which may originate throughout the brainstem and cerebellum, on the left (*lb*) and right (*rb*).

Network connectivity reflects the known anatomy of the mammalian VOR (Wilson and Melvill Jones 1979; Buttner-Ennever 1988). To represent the VOR relay, input project to hidden units and hidden project to output units. The hidden-to-output connection weights are initially fixed, because it is generally believed that plastic changes occur only at the VN (Galiana et al. 1984). The fixed weights to the outputs, of absolute value 0.50, have a crossed, reciprocal pattern (Table 1A). Left hidden units are inhibitory to *lr* and excitatory to to *mr*, while right hidden units have the opposite output projection pattern. Recurrent connections occur between hidden units on opposite sides of the brainstem. Because the vestibular commissures are inhibitory in mammals, the weights of the recurrent connections are constrained to be zero or less. Bias connection weights are initially fixed at zero to the outputs and at -1.00 to the hidden units, to reflect inhibition by cerebellar Purkinje cells which project to the VN but not to the motoneurons. The bias units have constant states of 0.50.

Training the normal network

The simulations begin by training the network shown in Fig. 1, with both vestibular inputs intact (normal network), to produce the VOR with velocity storage (Anastasio 1991). The network was trained on dynamic input/desired-output trajectories using a recurrent back-propagation learning algorithm (Williams and Zipser 1989). Briefly, the algorithm finds the error between actual- and desired-outputs, and computes the gradient of this error in weight space. The gradient is then used to update the weight values in the direction of reduced error. The algorithm is continuous in the sense that learning occurs contemporaneously with the dynamic behavior of the network. Input and desired-output sequences correspond to canal afferent signals and motoneuron eye-velocity commands that underlie the horizontal VOR response to two impulse head rotational accelerations, one to the left and the other to the right. Each response sequence is 30 time steps (ticks) long; each tick equals 5 s.

Input and desired-output sequences for *rhc* and *lr* are shown in Fig. 2A (dotted and dashed, respectively). The sequences for *lhc* and *mr* (not shown) are the inverse of those for *rhc* and *lr*, respectively. Head acceleration to the right (ticks 31 through 60) excites *rhc* and inhibits *lhc*. The appropriate VOR eye movement to the left would be produced by excitation of *lr* and inhibition of *mr*. The opposite pattern obtains for head rotations to the left (ticks 1 through 30). Output

Table 1A. Learned weight matrix for the intact, horizontal vestibulo-ocular reflex (VOR) neural network model. This network was trained to produce motoneuron activations that are equal and opposite to canal afferent activations, effecting the VOR, but have time constants four times longer, reflecting velocity storage. *lb* and *rb*, left and right nonvestibular neurons (bias units); *lhc* and *rhc*, left and right horizontal canal afferents (input units); *lvn* and *rvn*, left and right vestibular nuclei neurons (hidden units); *lr* and *mr*, lateral and medial rectus muscle motoneurons of the left eye (output units); –, disallowed connection. Bias-to-hidden, bias-to-output and hidden-to-output weights were fixed during learning

from: to:	*lb*	*rb*	*lhc*	*rhc*	*lvn1*	*lvn2*	*rvn1*	*rvn2*
lvn1	−1.000	–	6.154	−5.340	–	–	−4.573	−0.964
lvn2	−1.000	–	5.274	−5.839	–	–	−0.868	−0.003
rvn1	–	−1.000	−5.759	6.723	−4.423	−1.288	–	–
rvn2	–	−1.000	−5.276	4.554	−0.644	−0.001	–	–
lr	0.000	–	–	–	−0.500	−0.500	0.500	0.500
mr	–	0.000	–	–	0.500	0.500	−0.500	−0.500

Table 1B. Learned weight matrix resulting from retraining following left hemilabyrinthectomy (removal of left input unit, *lhc*). Retraining wes terminated just after the network had learned to restore VOR gain, before any time constant lengthening (velocity storage) had recovered. Abbreviations as in Table 1. All allowed connections had modifiable weights

from: to:	*lb*	*rb*	*lhc*	*rch*	*lvn1*	*lvn2*	*rvn1*	*rvn2*
lvn1	−0.753	–	–	−5.166	–	–	−4.377	−0.811
lvn2	0.438	–	–	−5.027	–	–	−0.089	−0.041
rvn1	–	−5.453	–	4.976	−4.670	−2.464	–	–
rvn2	–	−4.452	–	2.918	−0.838	−0.725	–	–
lr	−2.413	–	–	–	−0.629	−1.217	2.376	1.446
mr	–	2.413	–	–	0.629	1.217	−2.376	−1.446

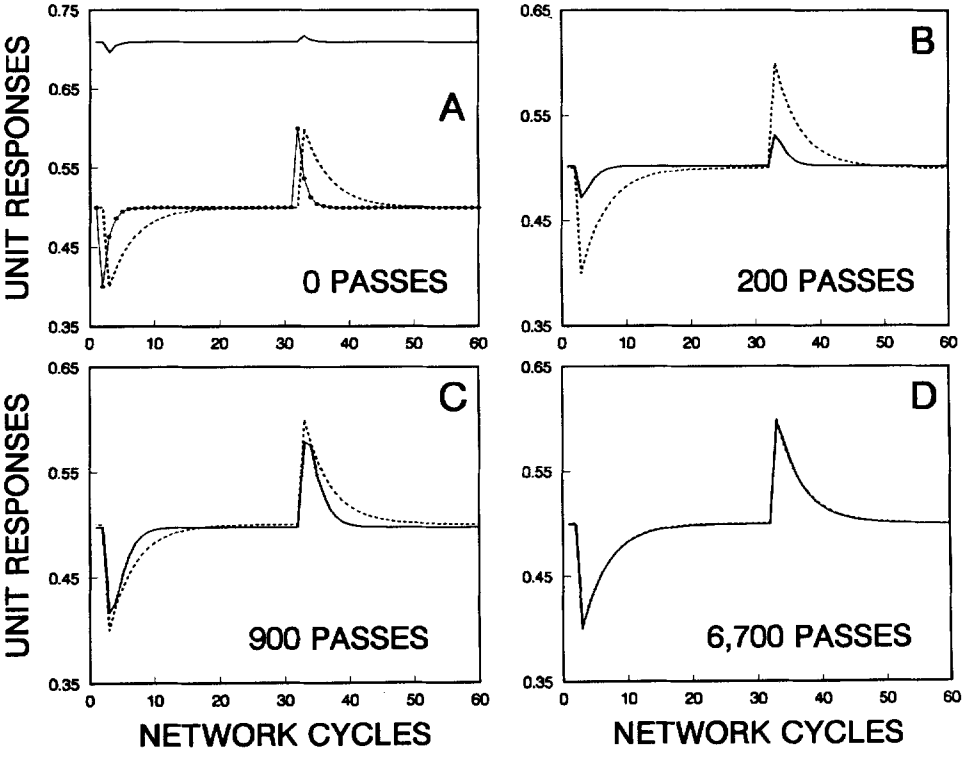

Fig. 2A–D. Simulated compensation in the VOR neural network model. Responses of output unit *lr* (solid) are shown at each stage of compensation, reached after increasing numbers of training sequency presentations (passes). Numbers of passes correspond to those in a network wherein only the weights at the hidden unit level are modifiable. **A** acutely following the lesion; **B** after spontaneous nystagmus has been eliminated; **C** after VOR gain has been largely restored; **D** after full recovery of VOR. Desired-output responses of *lr* (dashed) shown in all plots. Intact input from *rhc* (dotted) shown in **A** only

response magnitudes equal those of the inputs (gain of 1.00), signifying that VOR eye rotations should perfectly counterbalance head rotations. To reflect velocity storage, the output responses decay more slowly than the inputs, with time constants of four and one tick (20 and 5 s), respectively. A pure delay of one tick between input and output represents synaptic delay in the three-layered network. Between head movements, all inputs and desired-outputs have the same spontaneous rate (SR) of 0.50. With SRs balanced, no reciprocal eye velocity command is given and, consequently, no VOR eye movement is made.

The normal network learns the VOR transformation after about 4,000 training sequence presentations (passes); final weights are shown in Table 1A. The network develops reciprocal connections from input to hidden units, with *lhc* exciting and inhibiting left and right side hidden units, respectively; *rhc* has the opposite hidden unit projection pattern. This pattern reflects actual VOR organization (Wilson and Melvill Jones 1979) with the inhibitory connections corresponding to open-loop commissures. The recurrent connections, corresponding to closed-loop commissures, essentially form an integrating (*lvn1* and *rvn1*) and a nonintegrating (*lvn2* and *rvn2*) pair of hidden units (Anastasio 1991). The integrating pair subserve storage in the network. They have strong mutual inhibition and thus exert net positive feedback on themselves. The nonintegrating pair have almost no mutual inhibition but achieve time constant lengthening by coupling to the integrating pair. For both open- and closed-loop commissures, an inhibitory interneuron with unity gain is implied to satisfy Dale's law.

Unit responses are characterized by SR, gain and time constant. The SRs of hidden and output units are their responses between head movements, when both inputs (or just *rhc* in left hemilabyrinthectomized networks) are at 0.50. Gain is defined as the absolute value of the peak change from SR of any unit divided by the peak change from 0.50 of input unit *rhc*. Time constants are estimated by fitting single exponential curves to unit responses. In the fully trained, normal network, hidden units have lower SRs, higher gains, and longer time constants than the input units (Anastasio 1991).

Simulating vestibular compensation

After the normal network is trained, with both inputs intact, vestibular compensation can be simulated by removing the input from one side and retraining. Left hemilabyrinthectomy produces deficits in the model that correspond to those observed experimentally. Removal of *lhc* removes excitatory and inhibitory input to left and right hidden units, respectively, thereby decreasing left and increasing right hidden unit SRs. Due to the crossed hidden-to-output connections (Table 1A), this hidden unit SR imbalance causes a large increase and decrease in the SRs of *lr* and *mr*, respectively. The responses of output unit *lr* acutely following left input removal are shown in Fig. 2A (solid). Acutely, the SR of *lr* is greatly increased above normal (Fig. 2, dashed); that of *mr* (not shown) is decreased by the same amount. This output SR imbalance would result in eye movement to the left in the absence of head movement (spontaneous nystagmus). The gain of the outputs is greatly decreased. This is due to the removal of one half of the network input and to the SR imbalance forcing the output units into the low gain extremes of the squashing function. Velocity storage is also eliminated by left input removal, due to events at the hidden unit level (see below).

During retraining, only connections at the hidden layer (direct vestibular, open- and closed-loop commissural and bias) are modifiable, in accordance with the assumption of the previous model (Galiana et al. 1984). Hidden-to-output and bias-to-output connections remain fixed as in Table 1A. The relative time course of simulated compensation is similar to that observed experimentally. Spontaneous nystagmus is eliminated after 200 passes, as the SRs of the output units are brought back to their normal level (Fig. 2B). Output unit gain is largely restored by 900 passes, but time constant remains close to that of the inputs (Fig. 2C). At this stage, VOR gain has increased, but its time constant has remained low, indicating loss of velocity storage. This stage approximates the extent of experimantally observed compensation (Wolfe and Kos 1977; Maoioli et al. 1983; Fetter and Zee 1988). Completely restoring the normal VOR with full velocity storage requires over seven times more retraining (Fig. 2D). This compensatory time course is consistent with reduction of network error in that the stages bringing more error reduction occur sooner.

With the hidden-to-output connections fixed, synaptic changes underlying network compensation are constrained to occur at the hidden layer. The evolution in the strengths of synapses onto lesion-side hidden unit *lvn1* are shown in Fig. 3. The changes onto *lvn2 are*

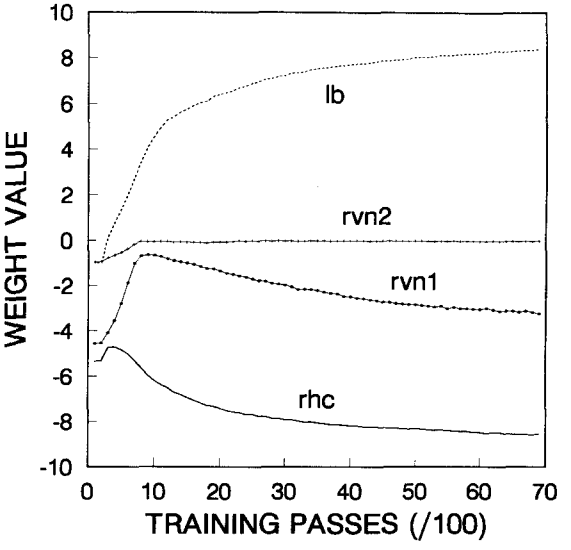

Fig. 3. Evolution of some weights during compensation in the VOR neural network model. Weights to lesion-side hidden unit *lvn1* are shown from the left bias unit *lb* (dashed), intact-side hidden units *rvn1* (dotted) and *rvn2* (scored) and intact canal afferent *rhc* (solid). Only weights at the hidden unit level are modifiable in this simulation

similar to those onto *lvn1*, while those onto intact-side hidden units (*rvn1* and *rvn2*) are essentially the opposite. Network balance is restored (and spontaneous nystagmus is eliminated) primarily by increases in excitatory and inhibitory bias to left and right hidden units, respectively. The inputs from the remaining canal (*rhc*), which are inhibitory to left and excitatory to right hidden units, initially decrease in absolute value, helping to rebalance hidden unit SRs bilaterally. Gain is subsequently recovered by redoubled increases in the strengths of the reciprocal inputs from *rhc*, which are balanced by increased bias. Overall, the closed-loop inhibitory commissural connections change little. The largest changes in these weights occur at the stage corresponding to physiological compensation (900 passes), where they increase slightly in absolute value to right hidden units, but decrease almost to zero to left hidden units (Fig. 3).

These results can be compared to those of the previous model (Galiana et al. 1984) that suggested that vestibular compensation can be mediated entirely by changes in the strengths of the closed loop commissures, and predicted that closed-loop commissural inhibition should be lower to the lesion-side than to the intact-side. In the current model, the learning algorithm did change the clossed-loop weights in the direction predicted by the previous model, but rather than using closed-loop weight changes alone, it effected compensation primarily with large changes in bias, direct vestibular and open-loop commissural connections. The current model cannot adequately compensate when the simulation is rerun with only the closed-loop commissures modifiable. Under this constraint, the algorithm manages to eliminate spontaneous nystagmus by decreasing closed-loop inhibition to zero to the lesion-side and increasing it by almost 20 times to the intact-side. However, the algorithm is incapable of both eliminating spontaneous nystagmus and increasing VOR gain using closed-loop commissures alone.

The changes in the closed-loop weights that are observed in the current model have dynamic consequences. The closed-loop commissures destabilize the network by integrating any imbalance between the VN bilaterally. Because imbalance constitutes the largest source of error, the adaptive network reduces the destabilizing effects of velocity storage by greatly diminishing the closed-loop connections to the lesion-side. To illustrate this, perturbing network balance by increasing *rb* produces almost twice as much spontaneous nystagmus at 6,700 passes, where closed-loop interactions have increased toward normal, than at 900 passes, where closed-loop connections to the lesion-side have decreased almost to zero.

Comparison to neurophysiological data

The neurophysiological veracity of the model can be assessed by comparing the responses of hidden units to the behavior of VN neurons in animals at various stages of compensation. The responses of the hidden units during each stage of simulated compensation are shown in Fig. 4A and C. In the normal network (NM stage, dotted), average hidden unit SR is 0.24 (Fig. 4A) and average gain is 2.56 (Fig. 4C). Acutely following left input removal (AC stage), the SRs of left (dashed)

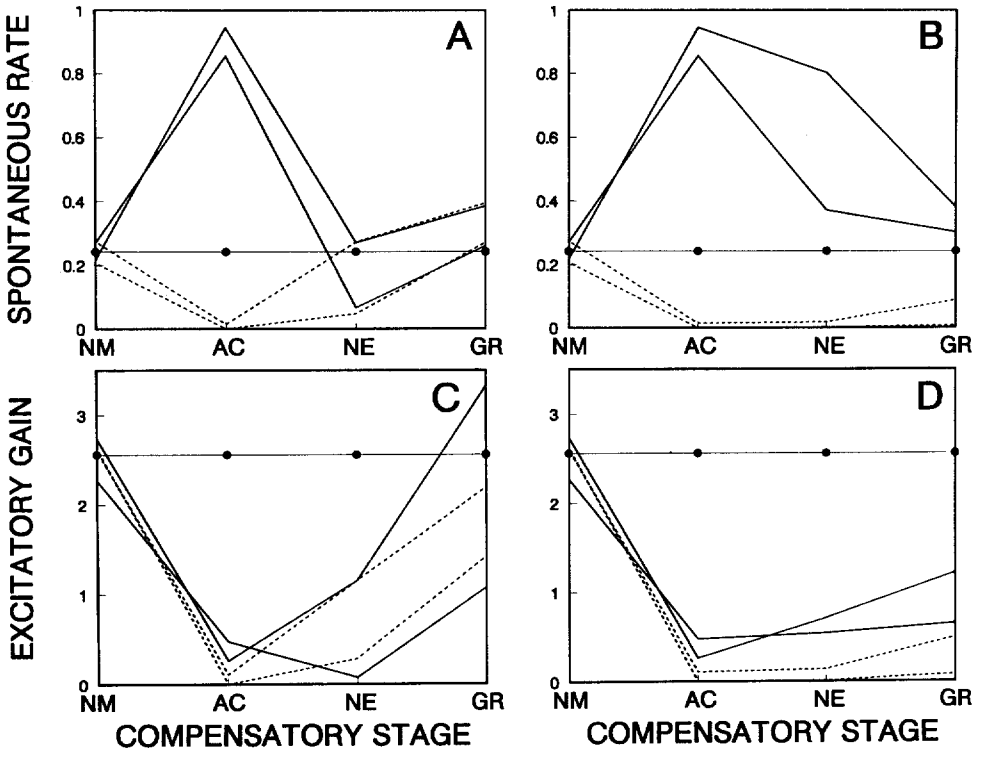

Fig. 4A–D. Behavior of hidden units at various stages of compensation in the VOR neural network model. Spontaneous rate (SR, **A** and **B**) and gain (**C** and **D**) are shown for networks with only hidden layer weights modifiable (**A** and **C**) or with all weights modifiable (**B** and **D**). Normal average SR (**A** and **B**) and gain (**C** and **D**) shown as dotted lines. NM: normal stage; AC: acutely following lesion; NE: after spontaneous nystagmus is eliminated; GR: after VOR gain is largely restored (but velocity storage has not recovered)

and right (solid) hidden units decrease and increase, respectively (Fig. 4A). One left hidden unit (*lvn1*) is actually silenced; *lvn1* is the left side member of the integrating pair that receives strong inhibition from the right side. Hidden unit gain at AC stage is greatly reduced bilaterally (Fig. 4C), as for the outputs.

At the point where spontaneous nystagmus is eliminated (NE stage), hidden units SRs are balanced bilaterally, and none of the units remain silent (Fig. 4A). When VOR gain is largely restored (GR stage, corresponding to physiological compensation), the gains of the hidden units have substantially increased (Fig. 4C). At GR stage, hidden unit SRs have also increased, but the average SRs of left and right hidden units are still equal; the bilateral SR balance has been strictly maintained (Fig. 4A).

The model represents so-called type I VN neurons, which respond in the same sense as the ipsilateral canal afferents from which they receive direct excitatory input (Wilson and Melvill Jones 1979). Type II VN neurons, which respond in the sense opposite to that of type I (ibid.), are implied in the network as the interneurons that mediate open- and closed-loop inhibition. Only data on type I VN neurons will be considered. A comparison reveals that the behavior of hidden units in this simulation (with hidden weights only modifiable) does *not* correspond to that observed for real VN neurons in compensated animals.

Neurophysiological data on VN neurons in normal and compensated animals have recently become available in a number of mammalian species (Precht et al. 1966; Yagi and Markham 1984; Ried et al. 1984; Hamann and Lannou 1988; Smith and Curthoys 1988ab; Newlands and Perachio 1990a). The results from the various studies differ somewhat, due perhaps to differences in surgical and pharmacological preparation (e.g. cerebellectomy, barbiturate anesthesia) that are known to affect compensation (Schaefer and Meyer 1974). All studies agree, however, that the number of active VN neurons on the lesion-side decreases acutely following hemilabyrinthectomy, and that many lesion-side VN neurons remain silent at the compensated stage (corresponding to GR in Fig. 4). Further, most studies agree that, acutely, the SRs of intact-side VN neurons increase above normal, while those of active lesion-side VN neurons decrease below normal, and that a bilateral imbalance in SR persists into the compensated stage. These findings are in sharp contradistinction to the model, where hidden unit SRs are balanced at the compensated stage and no units remain silent. Also, rather than substantially recovering gain as in the model, most studies agree that the gains of VN neurons in compensated animals increase little from their low values acutely following the lesion.

The reason why the network model adopts its particular (and unphysiological) solution to vestibular compensation is apparent from a consideration of network architecture (Fig. 1). With the hidden-to-output weights fixed, output unit responses are a direct reflection of hidden unit responses. Thus, output SRs will be balanced only if hidden SRs are balanced, and output gain will increase only if hidden gain increases. It is clear from the discrepancy between model and actual data that compensation cannot depend solely upon changes in synapses onto VN neurons.

Relaxing constraints

A better match between model and experimental data can be achieved by rerunning the compensation simulation with all network connections modifiable (Fig. 1). Bias-to-output weights are allowed to take on any value, while hidden-to-output weights are constrained to preserve their reciprocal pattern in sign, but can take on any absolute value. The time course of compensation in the all-weights-modifiable example is similar to the previous case (Fig. 2), but each stage is reached after fewer passes. VOR gain, but not velocity storage, is restored after 200 passes. Network weights at this stage (GR) of the all-weights simulation, which approximates the extent of physiological compensation, are given in Table 1B.

In the all-weights simulation, compensation can be produced by synaptic changes at the output as well as at the hidden units. Output SR is balanced (and spontaneous nystagmus is eliminated) by developing large excitatory and inhibitory bias weights to *mr* and *lr*, respectively. Similarly, output gain (and thus VOR gain) is restored by increases in the aboslute value of the reciprocal hidden-to-output connections. At the hidden level, bias weight changes are similar to the previous case but smaller, while reciprocal weights from *rhc* actually decrease slightly in absolute value. The closed-loop commissural weights change little to either side.

The behavior of the hidden units in the all-weights simulation is shown in Fig. 4B and D. The SRs and gains of hidden units in the normal (NM) and acute (AC) stages are reproduced from Fig. 4A and C, respectively. At NE stage, even though spontaneous nystagmus is eliminated, there remains a large bilateral imbalance in hidden unit SR, with left (dashed) and right (solid) hidden unit SRs lower and higher than normal, respectively (Fig. 4B). One lesion-side hidden unit (*lvn1*) remains silent. At GR stage, the bilateral SR imbalance persists, with *lvn1* still essentially spontaneously silent (Fig. 4B). Hidden unit gain at GR stage has increased only modestly from the low acute level (Fig. 4D). This small gain increase results primarily from hidden SRs being brought away from the low gain extremes of the squashing function; the gain of *lvn1* is negligible. The behavior of hidden units in the all-weights simulation (Fig. 4B and D) more closely matches that of actual VN neurons in compensated animals. This modeling result constitutes a testable prediction that synaptic plasticity may be occurring at the motoneurons as well as at the VN in vestibular compensation. This hypothesis does not exclude alternative mechanisms involving changes in separate pathways that are parallel to the main VOR pathway represented in the model (see below).

Network dynamics

In the acutely lesioned network, silencing of *lvn1* breaks the commissural interactions of the integrating pair and consequently eliminates velocity storage. Loss of velocity storage is advantageous for the network, because integration of the pathological VN imbalance caused by the lesion is prevented. Many real lesion-side VN neurons, possibly also inside closed inhibitory loops, are silenced by hemilabyrinthectomy (see above). This may serve as a fail-safe mechanism in the real VOR, essentially switching-off velocity storage in the event of large, bilateral VN imbalances.

During the compensatory process, the network with all weights modifiable has sufficient degrees of freedom to re-establish output balance and gain, without bringing *lvn1* back into its operating range. Keeping *lvn1* off helps the network compensate without the destabilizing effects of velocity storage. Similarly in compensated animals, many lesion-side VN neurons are permanently silenced, and VOR time constant remains low, indicating minimal recovery of velocity storage (see above). This raises the possibility that the real VOR maintains stability during and after compensation by keeping silent those lesion-side VN neurons that participate in closed inhibitory commissural loops and produce instability prone, velocity storage integration.

Loss of velocity storage in the model, in response to step head rotational acceleration stimuli, is shown in Fig. 5. The expected output step response is shown for *lr* in Fig. 5A (dashed). It consists of exponential rises and falls, with the longer VOR time constant, at step on-set and off-set, respectively. Instead of expressing the longer VOR time constant, the actual step response of *lr* in the all-weights compensated network at GR stage (Fig. 5A, dotted) has rise and fall time constants that are are equal to those of the canals, indicating complete loss of velocity storage. This loss is due to the behavior of the hidden units. The step responses of the integrating pair of hidden units in the all-weights compensated network are shown in Fig. 5B (*lvn1*, lower dotted; *rvn1*, upper dotted). Velocity storage is eliminated because *lvn1* is silenced, and this breaks the closed-loop that lengthens the time constants of both hidden and output units.

Paradoxically, in the normal network with all hidden units active, the output step response rise time constant is also equal to that of the canal afferents. This is shown for *lr* in the normal network in Fig. 5A (solid). The step responses of the hidden units in the normal network are shown in Fig. 5B (*lvn1*, dashed; *rvn1*, solid). Unit *lvn1* is quickly driven into cut-off by the step stimulus. This breaks the closed-loop and eliminates velocity storage, accounting for the short rise time constants of hidden and output units. The opposite occurs at stimulus termination. Unit *lvn1* comes out of rectification, thereby reactivating velocity storage, which then prolongs the fall time constants of hidden and output units as the network relaxes from the reciprocal initial condition in which it is left after the step.

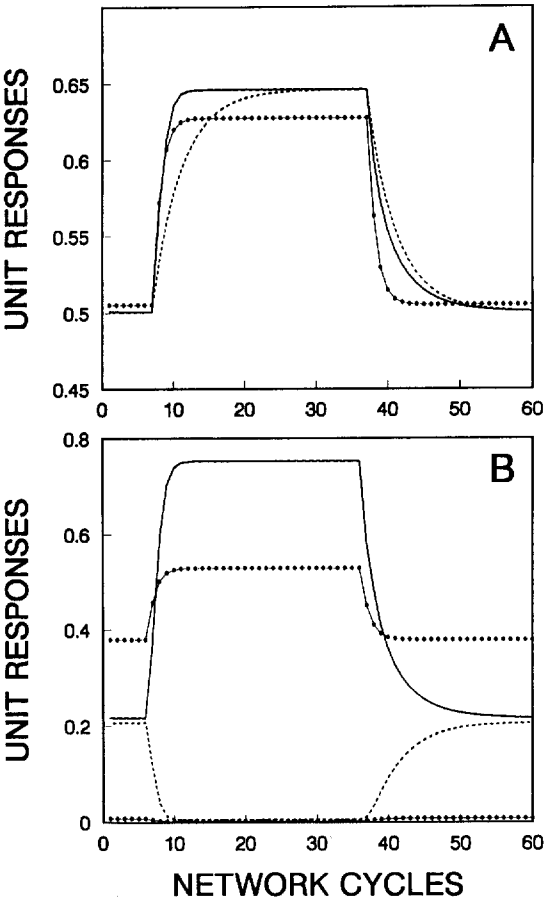

Fig. 5A, B. Responses of units to step head rotational acceleration stimuli in the VOR neural network model. **A** expected response of *lr* with VOR time constant (dashed), and actual responses of *lr* in normal (solid) and all-weights compensated (dotted) networks. **B** response of *lvn1* (dashed) and *rvn1* (solid) in normal network, and of *lvn1* (lower dotted) and *rvn1* (upper dotted) in all-weights compensated network. The all-weights compensated network has reached the stage corresponding to physiological compensation, where spontaneous nystagmus has been eliminated and VOR gain largely restored, but velocity storage has not recovered

These modeling results can explain some conflicting experimental findings concerning the dynamics of VN neurons in normal and compensated animals. The time constants of VN neurons were found to be shorter in compensated than in normal gerbils for low frequency sinusoidal responses (Newlands and Perachio 1990a), but not for step on-set responses in cats (Yagi and Markham 1984). Rather than being a species difference, the disagreement may involve the type of stimulus used.

Step accelerations are intense stimuli that can drive VN neurons to extreme levels. In response to a step in their off-directions, many VN neurons in normal cats were observed to rectify (ibid.). As shown in Fig. 5, this would disrupt commissural interactions and reduce velocity storage and VN neuron rise time constants, just as if those rectifying neurons were silenced as they are in compensated animals. In fact, VN neuron rise time constants were observed to be short in both normal and compensated cats, and equal to about four seconds in

both cases (ibid.). This time constant matches that of canal afferents in cats (Ezure et al. 1978), indicating loss of velocity storage in step rise responses in both normal and compensated animals.

In contrast, sinusoidal stimuli that cause VN neuron rectification in normal animals can do so only near the peaks. Thus velocity storage and time constant are reduced more at the peaks than midrange (Anastasio 1991). In response to low frequency sinusoidal stimuli, with peak accelerations in the same range as the step stimuli used in the cat study above, many VN neurons in normal gerbils were also observed to rectify (Newlands and Perachio 1990a). However, because the data were subjected to analyses that took account of the entire response waveform (ibid.), velocity storage occurring midrange in normal animals would have registered. Time constants therefore would be longer in normal than in compensated gerbils, where velocity storage was presumably eliminated at all times due to VN neuron silencing (ibid.). The difference in time constants in normal and compensated networks grows larger as the intensity of the sinusoidal stimuli, and hidden unit rectification at peak, are reduced. This suggests that larger differences in VN neuron time constants in normal and compensated gerbils would have been observed if lower intensity sinusoidal stimuli had been used.

The normal nonlinear response to step stimuli may confer an advantage. Most head rotations probably begin with a short step acceleration, followed by a period of constant velocity. At step on-set, rectification of off-direction VN neurons that participate in closed commissural loops would switch-off velocity storage, allowing the VOR to respond to its canal input with minimum time constant. After the step, those neurons would be reactivated, switching velocity storage back on. This would maintain the VOR response during the period of constant velocity, the period during which the canals become inactive.

Such a difference in rise and fall time constants has been observed for VN neurons in monkeys (Waespe and Henn 1979). Fall time constants following step accelerations were found to range from ten to 25 s, reflecting velocity storage. In contrast, rise time constants at step on-set were shorter than five seconds for more intense stimuli, bringing them well within the range of canal afferent time constants in monkeys (Buttner and Waespe 1981). This indicates that velocity storage had been completely inactivated during the rising phase of the VN neuron response to the more intense step stimuli, and reactivated again during the falling phase.

Experimental considerations

Vestibular compensation is simulated using a recurrent back-propagation learning algorithm. It is unlikely that the algorithm used here corresponds to an actual, neurophysiological learning mechanism (Williams and Zipser 1989). However, the learning algorithm and real vestibular compensation share a critically important goal: the reduction of error. The model closely approximates actual compensation, and offers testable predictions so that it can, in any case, be subjected to experimental verification.

One important difference between the real compensated VOR and the model is that the former is asymmetrical. Following compensation for hemilabyrinthectomy, real VOR gain is always higher for head rotations to the intact-side (Wolfe and Kos 1977; Maioli et al. 1983; Fetter and Zee 1988). It may be that the extent of synaptic plasticity is limited for actual compensation. Asymmetries could also be simulated in the model by limiting connection weights. However, arbitrary weight controls defeat the purpose of using a learning algorithm. The model is constrained only to conform it to known anatomy; the algorithm is otherwise free to modify connection weights according to the gradient descent of error.

The fully adaptive model makes only small changes in both open- and closed-loop commissural weights, suggesting that the commissures may play a minor role in compensation. This conjecture, also developed in other recent models (Fetter and Zee 1988; Newlands and Perachio 1990b), has experimental support. The efficacy of inhibitory commissural connections, gauged from the responses of lesion-side type I VN neurons to electrical stimulation of the intact labyrinth, has been compared in normal and compensated cats. Although an earlier study found an increase in commissural efficacy after compensation (Precht et al. 1966), a more recent study failed to confirm this finding (Reid et al. 1984). In a more striking demonstration, compensation of postural deficits following hemilabyrinthectomy was observed to occur in commissurotomized rodents (Smith et al. 1986).

The model predicts that synaptic plasticity occurs at the motoneuron level in compensation. An alternative, but not exclusive, hypothesis is that compensation is effected by changes in a separate pathway that is parallel to the main VOR pathway represented in the model. This is possible considering that the other brain areas, such as the cerebellum, cerebellar nuclei and inferior olive, are also involved in the compensatory process (Schaefer and Meyer 1974; Llinas and Walton 1979). However, the existence of alternative hypotheses should not preclude experimental verification of the parsimonious prediction of the model.

The model predicts that both excitatory and inhibitory inputs from the VN onto motoneurons should increase in efficacy during compensation. This prediction could be tested by comparing eye movement or motoneuron responses to electrical stimulation of either of the VN before and after compensation. The model also predicts increases in excitatory and inhibitory bias to motoneurons that were excited and inhibited, respectively, by relays from the lesioned labyrinth. These bias changes will be more difficult to test directly because the site (or sites) of nonvestibular input to motoneurons have not been identified. It is also possible that bias is set by some mechanism intrinsic to the motor

nuclei or to the motoneurons themselves. Bias effects, however, may be testable indirectly by pharmacological means.

Acknowledgements. Special thanks to Drs. E. L. Keller and C. von der Marlsburg for comments and to A. A. Perachio for reviewing the manuscript. This work was supported by a grant from the Whitaker Foundation.

References

Anastasio TJ (1991) Neural network models of velocity storage in the horizontal vestibulo-ocular reflex. Biol Cybern 64:187–196

Blair SM, Gavin M (1981) Brainstem commissures and control of time constant of vestibular nystagmus. Acta Otolaryngol 91:1–8

Buttner U, Waespe W (1981) Vestibular nerve activity in the alert monkey during vestibular and optokinetic nystagmus. Exp Brain Res 41:310–315

Buttner-Ennever JA (1988) Neuroanatomy of the oculomotor system. Elsevier, Amsterdam

Ezure K, Schor RH, Yoshida K (1978) The response of horizontal semicircular canal afferents to sinusoidal rotation in cat. Exp Brain Res 33:27–39

Fetter M, Zee DS (1988) Recovery from unilateral labyrinthectomy in rhesus monkey. J Neurophysiol 59:370–393

Galiana HL, Flohr H, Melvill Jones G (1984) A reevaluation of intervestibular nuclear coupling: its role in vestibular compensation. J Neurophysiol 51:242–259

Hamann K-F, Lannou J (1988) Dynamic characteristics of vestibular nuclear neurons responses to vestibular and optokinetic stimulation during vestibular compensation in the rat. Acta Otolaryngol [Suppl] 455:1–19

Llinas R, Walton K (1979) Vestibular compensation: a distributed property of the central nervous system. In: Asanuma H, Wilson VJ (eds) Integration in the nervous system. Igaku Shoin, Tokyo, pp 145–166

Maioli C, Precht W, Ried S (1983) Short- and long-term modifications of vestibulo-ocular response dynamics following unilateral vestibular nerve lesions in the cat. Exp Brain Res 50:259–274

Newlands SD, Perachio AA (1990a) Compensation of horizontal canal related activity in the medial vestibular nucleus following unilateral labyrinth ablation in the decerabrate gerbil. I. type I neurons. Exp Brain Res 82:359–372

Newlands SD, Perachio AA (1990b) Compensation of horizontal canal related activity in the medial vestibular nucleus following unilateral labyrinth ablation in the decerebrate gerbil. II. type II neurons. Exp Brain Res 82:373–383

Precht W, Shimazu H, Markham CH (1966) A mechanism of central compensation of vestibular function following hemilabyrinthectomy. J Neurophysiol 29:996–1009

Raphan Th, Matsuo V, Cohen B (1979) Velocity storage in the vestibulo-ocular reflex arc (VOR). Exp Brain Res 35:229–248

Ried S, Maioli C, Precht W (1984) Vestibular nuclear neuron activity in chronically hemilabyrinthectomized cats. Acta Otolaryngol 98:1–13

Rumelhard DE, Hinton GE, Williams RJ (1986) Learning internal representations by error propagation. In: Rumelhard DE, McCleland JL, PDP Research Group (eds) Parallel distributed processing: explorations in the microstructure of cognition, vol 1: Foundation. MIT Press, Cambridge, pp 318–362

Schaefer KP, Meyer DL (1974) Compensation of vestibular lesions. In: Kornhuber HH (ed) Handbook of sensory physiology vol. VI/2. Springer, Berlin Heidelberg New York, pp 463–489

Smith PF, Curthoys IS (1988a) Neuronal activity in the contralateral medial vestibular nucleus of the guinea pig following unilateral labyrinthectomy. Brain Res 444: 295–307

Smith PF, Curthoys IS (1988b) Neuronal activity in the ipsilateral medial vestibular nucleus of the guinea pig following unilateral laybrinthectomy. Brain Res 444:308–319

Smith PF, Darlington CL, Curthoys IS (1986) Vestibular compensation without brainstem commissures in the guinea pig. Neurosci Lett 65:209–213

Waespe W, Henn V (1979) The velocity response of vestibular nucleus neurons during vestibular, visual, and combined angular acceleration. Exp Brain Res 37:337–347

Williams RJ, Zipser D (1989) A learning algorithm for continually running fully recurrent neural networks. Neural Comp 1:270–280

Wilson VJ, Melvill Jones G (1979) Mammalian vestibular physiology. Plenum Press, New York

Wolfe JW, Kos CM (1977) Nystagmic responses of the rhesus monkey to rotational stimulation follwing unilateral laybrinthectomy: final report. Trans Am Acad Ophthalmol Otolaryngol 84: 38–45

Yagi T, Markham CH (1984) Neural correlates of compensation after hemilabyrinthectomy. Exp Neurol 84:98–108

Dr. Thomas J. Anastasio
University of Illinois
Beckman Institute
405 North Mathews Avenue
Urbana, IL 61801
USA